Are your MRI contrast agents cost-effective?
Learn more about generic Gadolinium-Based Contrast Agents.
FRESENIUS KABI
caring for life

AJNR

Human germinal matrix: venous origin of hemorrhage and vascular characteristics.

H S Ghazi-Birry, W R Brown, D M Moody, V R Challa, S M Block and D M Reboussin

AJNR Am J Neuroradiol 1997, 18 (2) 219-229
http://www.ajnr.org/content/18/2/219

This information is current as of April 19, 2024.

Human Germinal Matrix: Venous Origin of Hemorrhage and Vascular Characteristics

Hani S. Ghazi-Birry, William R. Brown, Dixon M. Moody, Venkata R. Challa, Steven M. Block, and David M. Reboussin

PURPOSE: To examine the vascular supply and architecture of the germinal matrix in the preterm neonatal brain and to determine whether veins or arterioles are the source of germinal matrix hemorrhage. **METHODS:** Brains from eight preterm neonates (24 to 35 weeks' gestation) and two full-term infants were fixed in alcohol, embedded in celloidin, sectioned at 100- and 500-μm thicknesses, stained for alkaline phosphatase, and examined with light microscopy. High-resolution contact radiographs of 500-μm-thick sections were also mounted on glass slides for microscopic examination. **RESULTS:** The upper and middle regions of the germinal matrix are supplied by branches of the lateral striate arteries, whereas the inferior part is supplied by branches of the recurrent artery of Heubner. In brain sections from four of the preterm infants, we found 15 circumscribed hemorrhagic foci within the germinal matrix. The largest was 5 mm in diameter; the smallest, 1 mm. All hemorrhages but one were closely associated with veins, with significant involvement of the perivenous space. The other hemorrhage appeared to be associated with an arteriole. In term and preterm infants, we found no arteriolar-to-arteriolar shunts, precapillary arteriolar-to-venules shunts, or vascular rete. At all gestational ages, the terminal vascular bed had only conventional branchings and connections. **CONCLUSION:** In preterm neonates, staining for endogenous alkaline phosphatase allows visual differentiation between afferent and efferent vessels. Germinal matrix hemorrhage in preterm neonates is primarily venous in origin. A hemorrhage can tunnel along the venous perivascular space, collapsing the vein and rupturing the tethered connecting tributaries. Extravasation of blood from the arterial circulation appears to be much less common.

Index terms: Cerebral hemorrhage; Infants, newborn; Pathology

AJNR Am J Neuroradiol 18:219–229, February 1997

Hemorrhages involving the neonatal brain are among the most frequent and serious events affecting the newborn. Although subdural hematoma was formerly the most common type of intracranial hemorrhage, probably as a result of adverse obstetric conditions, more recent data show a considerable decline in the proportion of such lesions and a corresponding marked increase in the frequency of germinal matrix hemorrhage (1). The primary reasons for this change are the marked reduction in the number of subdural hematomas resulting from improved obstetric management of the second stage of labor and a relative increase in cases of germinal matrix hemorrhage associated with the increased survival of premature infants with very low birth weight, who are supported by advanced neonatal intensive care. Currently, germinal matrix hemorrhage is the most frequent and important brain abnormality in the neonatal period.

Germinal matrix hemorrhage occurs primarily but not exclusively in premature neonates of very low birth weight. The recent large multicenter study coordinated by the National Institute of Child Health and Human Development

Received May 20, 1996; accepted after revision August 19.

Supported by NIH NS20618 Jacob K. Javits Neuroscience Investigator Award (D.M.M.) and the March of Dimes Birth Defects Foundation Grant #6-FY95–223 (W.R.B.).

From the Department of Radiology (H.S.G-B., W.R.B., D.M.M.), the Program in Neuroscience (W.R.B., D.M.M.), the Department of Pathology (W.R.B., V.R.C.), the Department of Pediatrics (S.M.B.), and the Department of Public Health Sciences (D.M.R.), Bowman Gray School of Medicine of Wake Forest University, Winston-Salem, NC.

Address reprint requests to Dixon M. Moody, MD, Department of Radiology, Bowman Gray School of Medicine, Medical Center Blvd, Winston-Salem, NC 27157.

AJNR 18:219–229, Feb 1997 0195-6108/97/1802–0219

© American Society of Neuroradiology

reported a 45% overall occurrence rate for germinal matrix hemorrhage in preterm low-birth-weight neonates (2). Since premature infants made up 9.7% of live-born infants in the United States in 1988, approximately 400 000 premature births would have occurred in 1995, and 40 000 of such infants would weigh less than 1500 g at birth; neonates with germinal matrix hemorrhage therefore constitute an enormous medical, social, and financial challenge for the nation (3). Additionally, improved obstetric and neonatal techniques have led to the survival of a not-insignificant percentage of extremely premature neonates. Indeed, reports describing survival of premature neonates with gestational ages of 22 to 24 weeks are not infrequent, and such infants have the highest risk for germinal matrix hemorrhage. Moreover, a significant percentage of preterm neonates with germinal matrix hemorrhage eventually contract cerebral palsy, which is a consequence of germinal matrix hemorrhage, its complications, or the associated lesions of periventricular leukomalacia or periventricular hemorrhagic infarction (4). Therefore, the significance of this condition cannot be overemphasized.

To reduce the prevalence of germinal matrix hemorrhage, one must understand its pathogenesis, and to do so requires detailed knowledge of the anatomy of the vascular system within the germinal matrix in the preterm infant as well as knowledge of the vascular etiologic source of germinal matrix hemorrhage. At present, some speculate that the vascular source of germinal matrix hemorrhage in the premature infant of very low birth weight is venous (5–8), whereas others believe it is capillary or arterial (9–11). Precise description of neonatal brain vasculature, generally, and of the bleeding source, specifically, has remained elusive because of the difficulty in classifying the immature vascular structures in the germinal matrix. In the deep brain microvasculature of the premature infant, it is difficult to identify supporting wall tissue (collagen in veins, smooth muscle in afferent vessels). The cause of germinal matrix hemorrhage cannot be established definitively without first classifying vessels into functional categories (ie, arterioles, capillaries, or veins) histologically. Although certain large, immature vessels in the germinal matrix seem to be implicated in germinal matrix hemorrhage, their morphologic status remains obscure, and investigators have classified them variously with such noncommittal terms as *vessels, sinusoids,* or *channels*.

One method for differentiating venous from arterial vessels is alkaline phosphatase histochemical staining. This research procedure, formerly used for the study of normal adult angioarchitecture, has been used to investigate adult vascular-based central nervous system abnormalities and to study brain vascular morphology in preterm neonates of very low birth weight (12). In the present study we used alkaline phosphatase histochemical staining and other techniques to identify various characteristics of the vascular supply and architecture of the germinal matrix in the brain of these preterm, low-birth-weight infants. Our purpose was to determine whether the large germinal matrix channels are venules, arterioles, or capillaries and to ascertain which types of vessels are the source of the germinal matrix hemorrhage.

Materials and Methods

Materials

We studied brains obtained at autopsy from eight preterm neonates of very low birth weight (postconception ages, 24 to 35.5 weeks) and from two full-term infants. Four of the preterm neonates had clinical diagnoses of germinal matrix hemorrhage, which were subsequently confirmed with pathologic examination of the brain. Typically, various combinations of the following prenatal risk factors and postnatal clinical abnormalities were present and may have contributed to the demise of the patients: maternal drug abuse, maternal insulin-dependent diabetes mellitus, antepartum hemorrhage, uteroplacental insufficiency, respiratory distress syndrome, hyaline membrane disease, pneumothoraces, severe hypoxia, hypercapnia, acidosis, severe hypotension, prolonged bradycardia, sepsis, anemia, thrombocytopenia, and other complications of prematurity. Both full-term infants died as a consequence of congenital heart malformations and associated complications. Details of gestational and postconception ages at death, birth weight, brain weight, Apgar scores, and germinal matrix hemorrhage grade for each patient are presented in the Table.

Methods

Immediately after autopsy, the neonatal brains were placed in cold 70% alcohol for at least 10 days for fixation. Formalin fixation was avoided because it destroys the endogenous alkaline phosphatase used by our staining technique. Subsequently, a whole-brain slice approximately 1 cm thick, incorporating both hemispheres, was obtained from each brain at and posterior to the foramen of Monro and included the thickest mass of germinal matrix

Demographic data and germinal matrix hemorrhage (GMH) status

Patient	Birth Weight, g	Gestational/ Postconception* Age, wk	Apgar Score†	Brain Weight, g	GMH Present	GMH Grade‡
1	550	24/24	2/5	76	Yes	II
2	660	24/24	1/2	52	No	· · ·
3	635	24/33	2/7	180	Yes	II
4	760	26/26	1/6	96	Yes	III
5	454	28/28	5/6	88	No	· · ·
6	1310	29/29	· · ·	185	No	· · ·
7	1480	31.5/32.5	1/3	220	Yes	II
8	3250	35/35.5	2/2	280	No	· · ·
9	2870	38/38.5	8/8	330	No	· · ·
10	3300	40/43	9/9	420	No	· · ·

* Postconception age at death.

† Apgar scores are at 1 and 5 minutes; patient 6 was born at home, so no score was available.

‡ GMH grade is according to the criteria of Papile et al (20).

as well as basal ganglia, thalamus, centrum semiovale, and cortex. The brain slices were then dehydrated in ascending grades of ethanol, embedded in celloidin, and serially sectioned at 100 μm, and 500 μm on a base sledge microtome. The celloidin allowed thick sections to be cut uniformly without cracking or distorting this delicate and fragile immature brain tissue. The sections were stained for native endothelial alkaline phosphatase by Bell and Scarrow's modification (13) of the Gomori method (14). The technique consists of incubating the sections in a medium containing calcium chloride and glycerophosphate. The endothelial alkaline phosphatase, which is still active after this fixation and dehydration, liberates phosphate radicals, which combine with the calcium ions to form calcium phosphate. Further incubations in solutions containing lead nitrate and then ammonium sulfide convert the invisible calcium phosphate into lead sulfide, which is brown to black. The sections are suitable for light microscopic observation after optional counterstaining, then mounting and coverslipping. Most of the usual neuropathologic stains can be used as the counterstain. Extensive segments of the vascular tree can be analyzed with the light microscope in thick (100 μm) celloidin sections.

The lead sulfide precipitate in the endothelium attenuates soft X-rays. Taking advantage of this property, high-resolution contact radiographs of the 500-μm-thick sections were made with an ISBR-60 microradiographic unit (Softex, Tokyo, Japan) using Kodak SO-343 film (Eastman-Kodak, Rochester, NY). The radiographs were cut out, mounted on glass slides with Eukitt mounting medium and coverslips, and examined with a light microscope.

The alkaline phosphatase staining technique as used in the present study produces a brown or black lead sulfide precipitate at the site of the ectoenzyme alkaline phosphatase. It has long been established, in human and other mammals, that the alkaline phosphatase stain occurs in the luminal and abluminal plasma membranes of endothelial cells of small arteries, arterioles, and capillaries, while veins are virtually unstained (13, 15–19). The veins are visualized by means of counterstains (eg, cresyl violet acetate/light green, Gill's hematoxylin). Our technique of differential visualization of afferent vessels from veins has been tested in different species and different organs and it has proved to be a reliable and robust procedure. The results of our alkaline phosphatase staining method have been independently validated in human and mammalian fetal tissue (15, 19). A potential limitation of this technique is that it requires many steps with careful attention to detail. For example, suitable incubation times in the lead nitrate solutions, which will not produce overstaining, must be determined, because in overstained tissues, the veins will also become stained. We found that the incubation times that are optimal for adult human brains were too long for neonatal brains. A further limitation of the alkaline phosphatase technique is that formalin fixation of the tissue destroys the enzymatic activity of alkaline phosphatase. Thus, formalin-fixed tissue cannot be used, including, of course, archived formalin-fixed tissues.

Results

Figure 1 shows the gross appearance of alkaline phosphatase–stained 100-μm-thick coronal sections containing material from both hemispheres of neonates with postconception ages of 24 weeks (Fig 1A) and 33 weeks (Fig 1B). As these sections show, we were able to harvest, section, process, and stain this delicate, immature brain tissue while preserving the tissue and maintaining its integrity. Afferent cerebral vessels (arteries, arterioles, and capillaries) stain densely with alkaline phosphatase, whereas efferent vessels (veins and venules) stain very lightly or not at all. Considerable reaction product was present in the corpus striatum and in the transcapsular caudolenticular gray striae because of *tissue* alkaline phosphatase (Fig 1A and B); however, such tissue

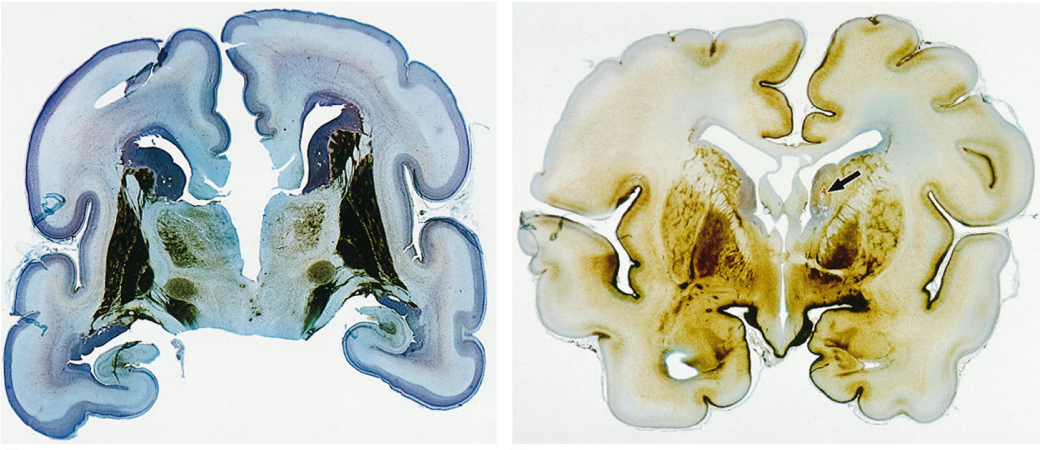

A B

Fig 1. *A*, Photomicrograph of a 100-μm-thick coronal section of the entire brain from a 24-week-postconception neonate (body weight, 550 g; brain weight, 76 g). The section was stained for endogenous alkaline phosphatase and counterstained with a cresyl violet acetate and light green. There is a prominent (blue) germinal matrix over the caudate nucleus. Note the good preservation and maintenance of tissue integrity of this very immature and friable brain (original magnification $\times$0.5).

B, Photomicrograph of a 100-μm-thick coronal section of the entire brain from a 33-week-postconception neonate (body weight, 635 g; brain weight, 180 g). The section was stained for alkaline phosphatase with no counterstain. Note the large hemorrhagic focus (*arrow*) in the left germinal matrix. This hemorrhage is thought to have occurred approximately 10 to 14 days before the infant's death (original magnification $\times$0.5).

alkaline phosphatase was separate and easily distinguishable from vascular alkaline phosphatase.

Vascular Characteristics of the Germinal Matrix in Low-Birth-Weight Neonates

Microscopic and microradiographic examination of alkaline phosphatase–stained whole-brain coronal sections from neonates of different gestational ages clearly demonstrated that the germinal matrix at the level of the foramen of Monro is supplied by arterioles arising from the recurrent artery of Heubner (Figs 2 and 3). This finding was evident where the rostrocaudal angle of the coronal sections paralleled the longitudinal axis of the artery of Heubner and its branches. When the origin of the vascular supply could not be observed on a particular section, observations from adjacent sections confirmed the vascular supply to this part of the germinal matrix.

More superiorly, at the region of the mid- and upper-caudate nucleus, terminal branches of the lateral striate arteries supplied the capillary bed of the germinal matrix (Fig 4). The germinal matrix tissue on the inferior surface of the corpus callosum derived its afferent blood supply from the terminal branches of the callosal penetrating arterioles. These vessels, like the recurrent artery of Heubner, arise from the anterior cerebral artery. Radiographic images of alkaline phosphatase–stained, thick (500 μm) celloidin sections provided an excellent overview of these vascular patterns (Figs 3 and 4).

The inferior region of the germinal matrix, which is supplied by branches of the recurrent artery of Heubner, was characteristically traversed by many arterioles coursing superiorly to supply their capillary network in the germinal matrix adjacent to the inferior portion of the caudate nucleus (Fig 2). This region of the germinal matrix was dominated by arterioles and capillaries; veins and venules were significantly fewer. In the midportion of the germinal matrix, the numbers of arterioles, capillaries, and thin-walled periventricular veins were approximately equal (Figs 2 and 5). In contrast, thin-walled veins outnumbered arterioles in the superior aspect of the germinal matrix. At the superior lateral angle of the lateral ventricle, the periventricular veins converge and connect with transcerebral medullary veins, which subsequently fan out toward the cerebral cortical surface (Fig 6). Venous blood can drain through these valveless veins either centripetally to the great vein of Galen or centrifugally to the leptomeningeal veins at the surface of the brain.

In several contiguous 100-μm-thick coronal sections of the brain samples, extrastriatal medullary arteries and arterioles could be traced from their superficial leptomeningeal origin to

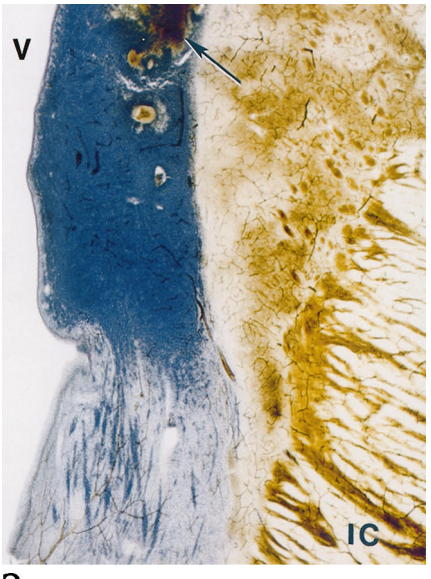

2

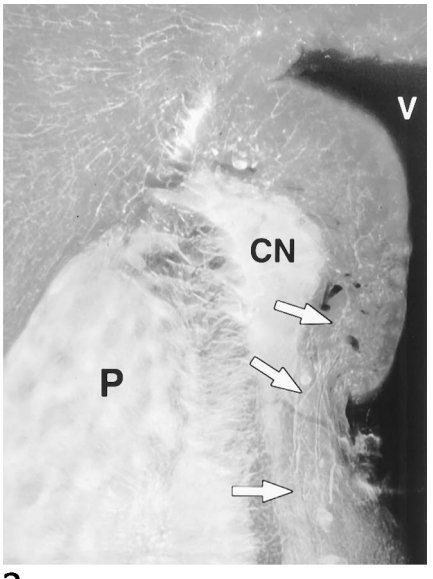

3

Fig 2. Vascular supply to germinal matrix. Celloidin alkaline phosphatase–stained coronal section, 100 μm thick, at the foramen of Monro from a 32.5-week-postconception very low birth weight premature infant with a grade II germinal matrix hemorrhage. The germinal matrix is stained blue, and the lateral ventricle is at the left margin of the illustration. Afferent microvessels stain brown because they have alkaline phosphatase in their endothelial cells. The inferior portion of the germinal matrix is fed by arterioles from the recurrent artery of Heubner, and in this area most of the arterioles are traveling upward to reach their capillary bed. More superiorly, fewer arterioles are found, and the veins are more plentiful. Several germinal matrix hemorrhages are seen in the perivascular spaces around the veins (*arrow* on largest). Furthermore, germinal matrix hemorrhage is more common in the mid-to-upper germinal matrix (top), where veins predominate, than in the inferior germinal matrix, where arterioles predominate. Unlike adults, this neonate has exuberant tissue alkaline phosphatase in the corpus striatum and internal capsule (*IC*), seen as the brown, nonvascular streaks on the right half of the illustration. The smallest vessels seen are capillaries. The ventricle (*V*) is to the left (cresyl violet acetate and light green counterstain, original magnification ×5) (from Moody et al [12]).

Fig 3. Microradiograph of 500-μm-thick alkaline phosphatase–stained coronal section from a 24-week-gestation neonate. Ascending branches of the recurrent artery of Huebner (*arrows*) supply the inferior and middle portions of the germinal matrix, whereas the superior portion of the germinal matrix is supplied by the lateral striate arteries (see Fig 4). The ventricle (*V*) is to the right. The brightness seen in the caudate nucleus (*CN*) and putamen (*P*) represents endogenous tissue alkaline phosphatase (original magnification ×2.5).

the germinal matrix deep in the core of the brain. The walls of these extrastriatal medullary vessels, as well as striatal arteries and arterioles, contained rudimentary smooth muscle, as identified by Gill's hematoxylin counterstain.

Clear differentiation between venous and arterial vessels with the alkaline phosphatase histochemical staining method facilitated analysis of connections between functionally different vessels in the microcirculation. In all neonatal brains, regardless of gestational age, no evidence was found of arteriolar-to-arteriolar or arteriolar-to-venous shunts or vascular rete. However, connections between arterioles via the continuous capillary bed were often observed (Fig 7). The terminal vascular bed had only conventional branchings and connections (ie, arteriole to capillary to postcapillary venule-to collecting venule to vein) (Figs 7 and 8).

Use of staining times established for adult brain tissues resulted in excessively strong alkaline phosphatase staining of the arteries, arterioles, and capillaries in the infants' brains; therefore, staining times were reduced. As stated earlier, considerable reaction product was present in the corpus striatum and in the transcapsular caudolenticular gray striae because of tissue alkaline phosphatase (Figs 1 and 4). This tissue alkaline phosphatase was clearly separate from vascular alkaline phosphatase. In a few instances, large periventricular veins in the germinal matrix also exhibited extremely faint alkaline phosphatase staining, which was easily distinguishable from the more marked dense staining in arterioles and capillaries (Fig 8). The veins were visible after counterstaining (Figs 5 and 8).

Vascular Characteristics of Germinal Matrix Hemorrhage

Four preterm very low birth weight neonates ranging in postconception age from 24 to 33 weeks, with a mean birth weight of 856 g and a mean brain weight of 143 g, had pathologically confirmed germinal matrix hemorrhage (Table). According to the classification method of Papile et al (20), three infants had grade II hemorrhages and one infant had a grade III lesion. No choroid plexus hemorrhage was identified.

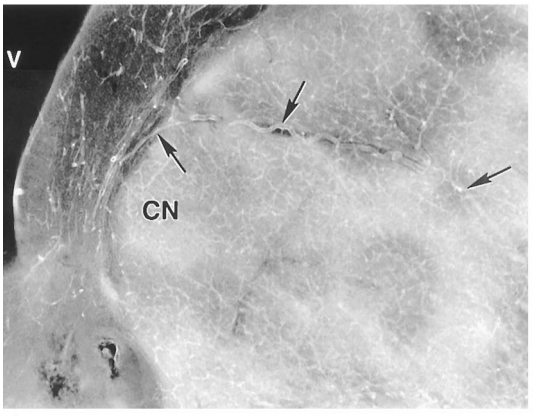

4

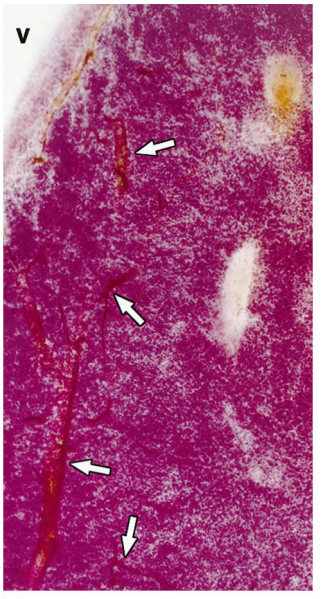

5

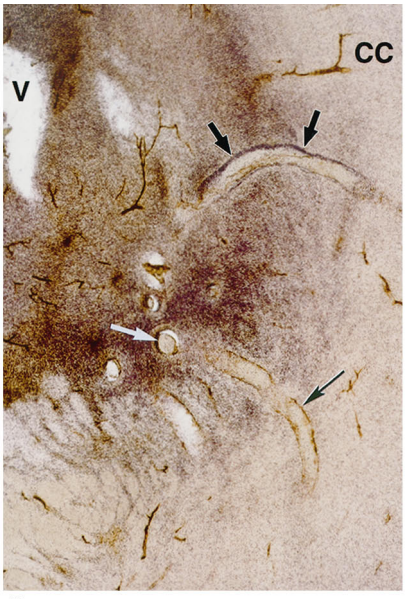

6

Fig 4. Microradiograph of a 500-μm-thick alkaline phosphatase–stained coronal section from a 31-week-gestation neonate. Distal branches of the lateral striate artery (*arrows*) ramify into the middle and superior portions of the germinal matrix over the head of the caudate nucleus (*CN*). The presence of modest tissue alkaline phosphatase in the corpus striatum, but not in the germinal matrix, produces a lighter background. The ventricle (*V*) is to the left (original magnification ×10) (from Moody et al [12]).

Fig 5. Multifocal venous germinal matrix hemorrhage. Celloidin section of the germinal matrix, 100 μm thick, with cresyl violet acetate and light green counterstain. In this middle region of the germinal matrix, the number of afferent vessels (*arrows*) was approximately equal to that on the venous side. Several venous hemorrhages are also seen as yellow-brown smudges widening the perivascular spaces (at the center and to the bottom). The alkaline phosphatase–stained arterioles and capillaries are not associated with the hemorrhage. The lateral ventricle (*V*) is in the upper left (original magnification ×25) (from Moody et al [12]).

Fig 6. Periventricular veins connect with medullary veins. Alkaline phosphatase–stained celloidin section, 100 μm thick, from a 32.5-week-postconception very low birth weight neonate (Fig 2), with cresyl violet acetate and light green counterstain. *V* indicates ventricle; *CC*, corpus callosum. Germinal matrix is dark cellular material to the bottom and left. Connections are seen between periventricular veins (*white arrow* on one example) and the transcerebral medullary veins (*thin black arrow* on one example). Such vessels may also drain medially toward the galenic drainage system. The dark material adjacent to these veins consists of germinal cells (*wide black arrows*) migrating outward, not vascular endothelial alkaline phosphatase reaction product. Note also that the only afferent (stained) vessels approaching the ventricles at this level are the smallest arterioles and capillaries (original magnification ×10) (from Moody et al [12]).

The mean survival time among three of the infants was 16 hours 20 minutes, whereas the fourth infant, born at 24 weeks' gestation, survived for 61 days. This infant had a grade II germinal matrix hemorrhage between postnatal days 47 and 54, an unusually late time for this event to occur.

Microscopic examinations of brain sections from the four patients showed 15 circumscribed hemorrhagic foci within the germinal matrix; the largest focus had a diameter of 5 mm and the smallest, 1 mm. All the hemorrhagic foci except one were either intricately associated with venous vessels or confined to the perivenous space (Figs 2, 5, and 9). The single nonconforming hemorrhagic focus was closely associated with an arteriole (Fig 10). The point at which the germinal matrix hemorrhage ruptured into the lateral ventricle was also observed in some cases (Fig 9). Fourteen (93%) of 15 of the hemorrhagic foci in the germinal matrix were very closely linked to veins. In some instances, a defect in the wall of the closely related vein, presumably the primary rupture point (ie, source of bleeding), could be clearly seen. Importantly, in a large number of cases, blood from the germinal matrix hemorrhage was seen tunneling along the perivenous space of a germinal matrix vein. This hemorrhagic invasion of the venous perivascular spaces appeared to compress the vein and cause tethering and rupture of smaller connecting venous tributaries (Figs 10–14). This phenomenon was never seen in association with arterioles or capillaries.

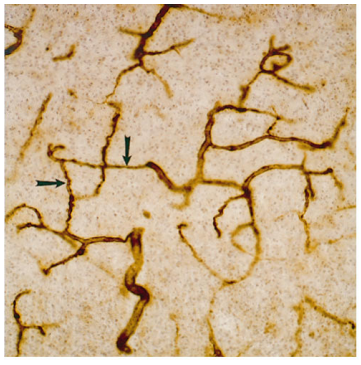

7

8

Fig 7. Continuous capillary bed. Alkaline phosphatase–stained coronal section, 100 μm thick, with cresyl violet acetate and light green counterstain. No unconventional connections were found between arterioles and veins or from arterioles to arterioles directly. The continuous capillary bed, in which arterioles connect to arterioles via capillaries (*arrows* on one example), was common throughout (original magnification ×25) (from Moody et al [12]).

Fig 8. Appearance of alkaline phosphatase–stained brain microvessels in a 32.5-week-postconception neonate. The surface of the brain is to the bottom and a medullary vein (*asterisk*) (lightly stained) in the center of the section is flanked by two medium-sized arterioles (*large arrows*) and their capillaries (densely stained). Note the continuous capillary network, which connects arterioles. The staining becomes much lighter at the junction of the capillary and the postcapillary venule (*small arrows*). There are no direct arteriovenous shunts without an intervening capillary network (100-μm-thick celloidin section, original magnification ×25).

In fact, all arterioles and capillaries that were traced histologically appeared normal. These vessels were seen in both the ependymal aspect and the lateral aspect of the hemorrhagic foci. Intact capillaries were traced in one brain to within 10 μm of the ependymal lining (Fig 5).

Discussion

In this study, the alkaline phosphatase method was used for staining the vessel walls of neonatal microvasculature located deep in the brain. This method has advantages over techniques that require staining of intravascular contents (ie, blood) or postmortem injection of barium, India ink, colored latex, or plastic. With the alkaline phosphatase method, the arterial side of the microvasculature stains, unlike the venous side, which does not. Thick specimens can be examined with light microscopy and even thicker ones with radiography. The background neural tissue can be examined with standard or special counterstains. There is no leaking of intravascular contents at the cut section surface to compromise the observations. Finally, vascular distortion, incomplete filling, air bubbles, aneurysms, rupture, and other artifacts of injection are avoided. This feature is extremely useful for detecting points of rupture in the vessel wall.

Characteristics of Germinal Matrix Vasculature

Because the use of the alkaline phosphatase staining technique in thick brain sections enables one to trace vessels for a relatively long distance, our investigation determined that the midportion and inferior portion of the germinal matrix at the level of the foramen of Monro are supplied by branches from the recurrent artery of Heubner, whereas more superior areas of the germinal matrix were supplied by branches of the lateral striate arteries. These findings confirm previous studies that used angiography and histology (21, 22). Furthermore, superior regions of the germinal matrix were dominated by thin-walled veins, whereas inferior regions contained mainly arterioles.

One important observation from the current study concerns the controversial issue of precapillary arteriolar-to-venous shunts (10, 23) or arteriolar-to-arteriolar anastomoses (21, 24). Although these vascular connections have been reported previously, they have not been detected in adult human brains in some studies despite vigorous attempts to do so (25). In the premature neonatal brain, Pape and Wigglesworth (10) described an "immature vascular rete in the subependymal matrix," and Nelson et al (22) described shunts between vascular channels in the cerebrum. Such vascular connections were not found in the brains of the premature neonates in the present study, and all intraparenchymal vascular anastomoses were of the conventional type (ie, arteriole to capillary to postcapillary venule to collecting venule to vein). Such shunts are considered common in skin and other organs, and communication between adjacent capillaries is well established in the adult human brain (25). However, in the premature neonates studied here, even when a capillary was connected to two

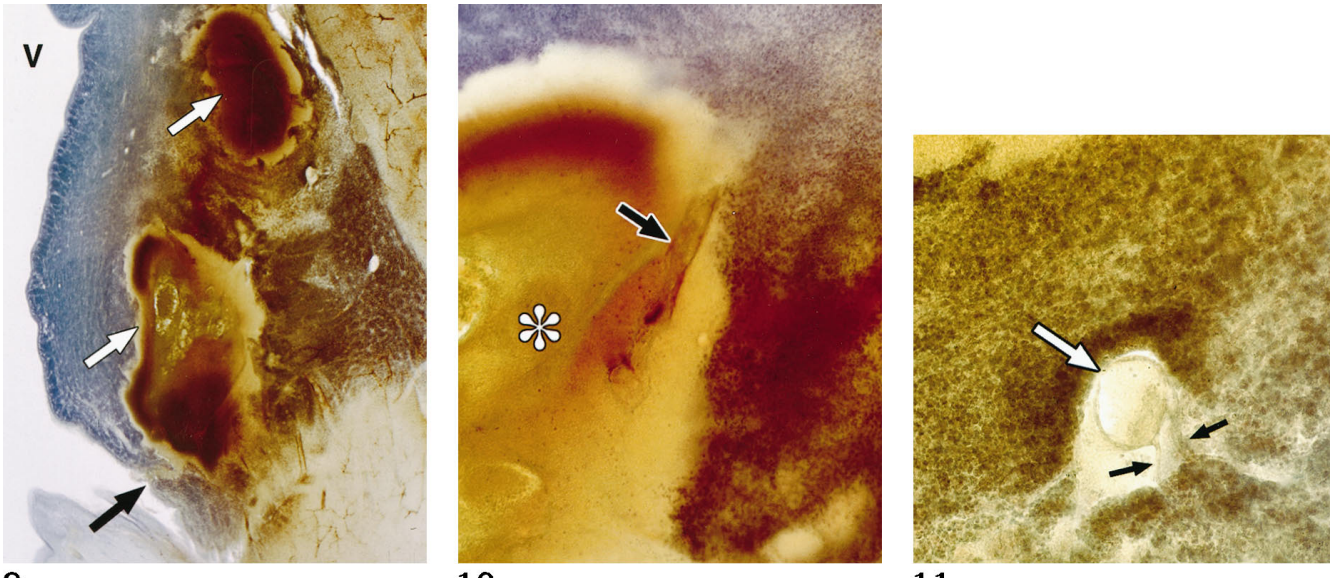

9 10 11

Fig 9. Celloidin alkaline phosphatase–stained coronal section, 100 μm thick, counterstained with cresyl violet acetate and light green from a 24-week-postconception very low birth weight premature neonate with a grade II germinal matrix hemorrhage. The germinal matrix (blue) is thickest over the caudate nucleus (top right) and shows multihemorrhagic sites (*white arrows*) within. The rupture point of the hemorrhage into the lateral ventricle (*V*), at the left margin of the illustration, is also shown (*black arrow*).

Fig 10. Celloidin alkaline phosphatase–stained 100-μm-thick section, counterstained with cresyl violet acetate and light green from a 24-week-postconception very low birth weight premature neonate with a germinal matrix hemorrhage. A germinal matrix hemorrhagic focus (*asterisk*) is seen surrounding an alkaline phosphatase–positive arteriole (*arrow*). Is the arteriole the source of the hemorrhage or an innocent bystander? (Original magnification $\times$25.)

Fig 11. Alkaline phosphatase–stained celloidin section, 100 μm thick, shows blood tunneling along the perivenous space of a germinal matrix vein seen in cross section. This appearance is never seen in association with arterioles or capillaries. Note that the wall of the vein is tethered by small tributaries (*black arrows*), and there appears to be a rupture site where it is believed that another tributary was torn away (*white arrow*) (original magnification $\times$50).

arterioles, it first had to pass a junction with a postcapillary venule. Therefore, intraparenchymal collateral flow is very likely to be weak and inefficient, as putative collateral flow selects the path of least resistance (ie, through a venule rather than the adjacent capillary). Capillary connections were observed, but arterial-to-venous shunts were not. Therefore, direct arterial-to-venous shunting of the cerebral blood, which would have been an important mechanism for transmitting arterial pressure directly to fragile periventricular germinal matrix veins, is unlikely to play a substantial role in the pathogenesis of germinal matrix hemorrhage.

Vascular Etiology of Germinal Matrix Hemorrhage

The present study involved four premature neonates of very low birth weight who had established germinal matrix hemorrhage. Although most of the hemorrhagic foci by far were located in the caudothalamic germinal matrix region adjacent to the foramen of Monro, one rather large hemorrhagic focus occurred in the temporal horns region of the germinal matrix. This location is consistent with the notion that germinal matrix hemorrhage occurs not only in the caudothalamic area but also in other germinal matrix regions, such as the temporal and occipital horns of the lateral ventricle and the cerebellar infratentorial region.

The data obtained here demonstrated that the overwhelming majority of hemorrhagic foci within the germinal matrix tissue were in proximity to venous vessels or confined within the perivenous space. Moreover, the venous vessels within the germinal matrix of the hemorrhagic cases were invariably distorted, and structural integrity of the veins was lost at or near the hemorrhagic foci. The distortion of the venous vessels probably reflects the phenom-

12

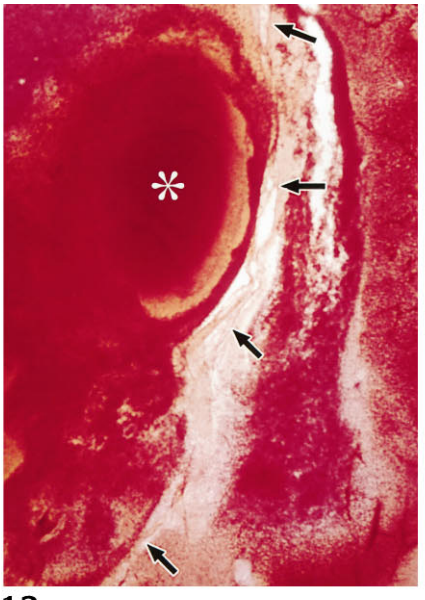

13

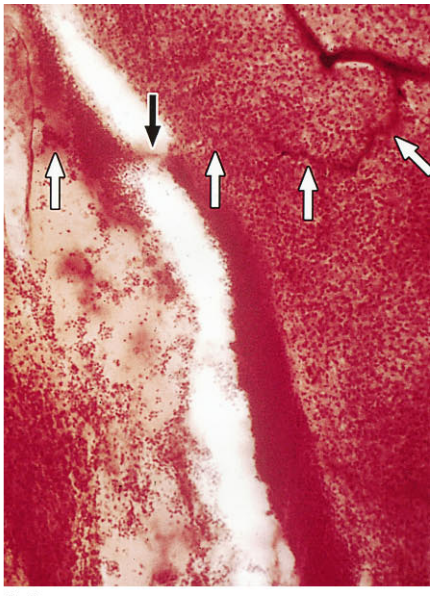

14

Fig 12. High-power magnification of alkaline phosphatase–stained celloidin section, 100 μm thick, with cresyl violet acetate and light green counterstain. This germinal matrix hemorrhage is situated in the perivenous space and surrounds a distorted periventricular vein (*arrowheads*). Two small unstained venous tributaries are seen entering this vein (*arrows*). The periventricular vein and the two tributaries can be distinguished from the afferent vessels by the lack of alkaline phosphatase staining. The hemorrhage dissecting along the perivenous space compresses this vein and is thought to increase parenchymal venous resistance. This phenomenon may lead to shearing off of the tributaries from the larger collecting vein. This appearance suggests a mechanism for further extension of germinal matrix hemorrhage (ie, tearing of the vessels crossing a hemorrhage in a perivascular space) (original magnification $\times$50) (from Moody et al [12]).

Fig 13. Germinal matrix hemorrhage in a 28-week-postconception neonate. Germinal matrix is to the left and caudate nucleus is to the right. There is a moderate-sized hemorrhage (*asterisk*). Blood is seen dissecting along the perivenous space and partially collapses the thalamostriate vein (*arrows*), which, at this stage, is an unstained germinal matrix sinusoid (alkaline phosphatase–stained 100-μm-thick celloidin section, original magnification $\times$10).

Fig 14. Stretched tributary to the germinal matrix sinusoid. This is a high-power view of the upper right corner of Figure 13. A stained arteriole is shown originating from a capillary (*arrows*), which crosses a hemorrhage-filled perivenous space to connect with the thalamostriate vein. Note how the alkaline phosphatase stain fades at the junction between the capillary and the postcapillary venule (original magnification $\times$25).

ena of stasis, thrombosis, and increase in central venous pressure before and after venous wall rupture. The point at which venous wall integrity is lost in the hemorrhagic cases is suggested to be the site of venous rupture and hemorrhage. That blood from the venous hemorrhage frequently tunnels along perivenous spaces surrounding distorted periventricular veins is important. The dissecting hemorrhage compresses the associated vein and is thought to increase parenchymal venous resistance, thereby leading to tethering and shearing off of small connecting venous tributaries. This likelihood is supported by the finding that, in some cases, smaller venous tributaries of larger veins were stretched and torn where blood had invaded the perivenous space and compressed the vein. The tethered and torn smaller venous tributaries are thought to provide a mechanism for further extension of germinal matrix hemorrhage.

Arterioles within the hemorrhagic foci in the germinal matrix, with one exception, appeared structurally and morphologically intact. In this one exception, the arteriole may not necessarily have been the primary source of hemorrhage, but could have been either an innocent bystander or a secondary hemorrhage. The fact that more than 93% of the hemorrhagic foci within the germinal matrix were closely associated with veins suggests that the vascular source leading to germinal matrix hemorrhage is predominantly venous. In the single case in which an arteriole was associated with a hem-

orrhagic focus, it was thought to represent a secondary event (see below).

The microvascular rupture point of germinal matrix hemorrhage remains controversial, in part because of the difficulty in identifying as either venules or arterioles the immature vessels found to be the source of the hemorrhage within the germinal matrix. In addition to these morphologic considerations, a number of physiologic etiologic mechanisms have been proposed for germinal matrix hemorrhage; these can be consistent with either one of the two theories of origin (ie, arterial or venous). The present investigation, using the unique alkaline phosphatase staining technique and thereby avoiding the problems associated with postmortem brain angiography, strongly supports the theory of venous origin suggested by Towbin (7), Volpe (8), Nakamura et al (6), and Moody et al (12). We propose that prematurity, its complications (such as respiratory distress syndrome), and treatment of these complications act upon the vulnerable germinal matrix veins to produce germinal matrix hemorrhage. The vulnerability of the germinal matrix veins stems from such characteristics as immature basal lamina, incomplete glial support, poor matrix support, and significantly increased transmural tension. Once venous hemorrhage is initiated, a cascade of events is likely to occur. Thus, we suggest that venous-derived blood in the germinal matrix mantle (*a*) increases tissue pressure and venous congestion and thereby leads to venous stasis and venous thrombosis; (*b*) distorts tissue cytoarchitectonics, thereby inducing tethering of venous tributaries and initiation of additional rupture points and further bleeding; and (*c*) induces tissue and venous congestion, which extrinsically compresses afferent vessels and obstructs arteriolar blood flow. Obstruction of arteriolar blood flow is likely to lead to vessel ischemia and hypoxia, to subsequent loss of arteriolar wall integrity, and finally to secondary arterial/arteriolar hemorrhage.

Acknowledgments

We thank Donna S. Garrison, PhD, for editorial assistance, Julianne R. Berckman for typing the manuscript, and Patricia Wood and Shirley Blackmore for expert technical assistance.

References

1. Levene MI, Williams JL, Fawer C-L. Ultrasound of the infant brain. *Clin Dev Med* 1985;92:1–144
2. Hack M, Horbar JD, Malloy MH, Tyson JE, Wright E, Wright L. Very low birth weight outcomes of the National Institute of Child Health and Human Development neonatal network. *Pediatrics* 1991;87:587–597
3. National Center for Health Statistics. *Vital Statistics of the United States, 1988, Vol 1: Natality*. DHHS Pub No. (PHS) 90–1100. Washington, DC: US Government Printing Office; 1990:257
4. Stanley FJ. The changing face of cerebral palsy? *Dev Med Child Neurol* 1987;29:263–265
5. Leech RW, Kohnen P. Subependymal and intraventricular hemorrhages in the newborn. *Am J Pathol* 1974;77:465–475
6. Nakamura Y, Okudera T, Fukuda S, Hashimoto T. Germinal matrix hemorrhage of venous origin in preterm neonates. *Hum Pathol* 1990;21:1059–1062
7. Towbin A. Cerebral intraventricular hemorrhage and subependymal matrix infarction in the fetus and premature newborn. *Am J Pathol* 1968;52:121–140
8. Volpe JJ. Intraventricular hemorrhage in the premature infant: current concepts, I. *Ann Neurol* 1989;25:3–11
9. Hambleton G, Wigglesworth JS. Origin of intraventricular haemorrhage in the preterm infant. *Arch Dis Child* 1976;51:651–659
10. Pape KE, Wigglesworth JS. Haemorrhage, ischaemia and the perinatal brain. *Clin Dev Med* 1979;69/70:11–38,100–132
11. Pasternack JF, Groothuis DR, Fischer JM, Fischer DP. Regional cerebral blood flow in the beagle puppy model of neonatal intraventricular hemorrhage: studies during systemic hypertension. *Neurology* 1983;33:559–566
12. Moody DM, Brown WR, Challa VR, Block SM. Alkaline phosphatase histochemical staining in the study of germinal matrix hemorrhage and brain vascular morphology in a very-low-birth-weight neonate. *Pediatr Res* 1994;35:424–430
13. Bell MA, Scarrow WG. Staining for microvascular alkaline phosphatase in thick celloidin section of nervous tissue: morphometric and pathologic applications. *Microvasc Res* 1984;27:189–203
14. Gomori G. Distribution of phosphate in normal organs and tissues. *J Cell Physiol* 1941;17:71–83
15. Scharrer E. A technique for the demonstration of the blood vessels in the developing central nervous system. *Anat Rec* 1950;107:319–327
16. Romanul FCA, Bannister RG. Localized areas of high alkaline phosphatase activity in the terminal tree. *J Cell Biol* 1962;15:73–84
17. Bannister RG, Romanul FCA. The localization of alkaline phosphatase activity in cerebral blood vessels. *J Neurol Neurosurg Psychiatry* 1963;26:333–340
18. Sanders RL, Bell MA. X-ray microscopy and histochemistry of the human cerebral blood vessels. *J Neurosurg* 1971;35:128–140
19. Norman MG, O'Kusky JR. The growth and development of microvasculature in human cerebral cortex. *J Neuropathol Exp Neurol* 1986;45:222–232
20. Papile L-A, Burstein J, Burstein R, Koffler H. Incidence and evolution of subependymal and intraventricular hemorrhage: a study of infants with birth weights less than 1,500 gm. *J Pediatr* 1978;92:529–534
21. Nakamura Y, Okudera T, Hashimoto T. Microvasculature in germinal matrix layer: its relationship to germinal matrix hemorrhage. *Mod Pathol* 1991;4:475–480
22. Nelson MD Jr, Gonzalez-Gomez I, Gilles FH. The search for human telencephalic ventriculofugal arteries. *AJNR Am J Neuroradiol* 1991;12:215–222
23. Hasegawa T, Ravens JR, Toole JF. Precapillary arteriovenous

anastomoses: "thoroughfare channels" in the brain. *Arch Neurol* 1967;16:217–224
24. Kuban KCK, Gilles FH. Human telencephalic angiogenesis. *Ann Neurol* 1985;17:539–548
25. Moody DM, Bell MA, Challa VR. Features of the cerebral vascular pattern that predict vulnerability to perfusion or oxygenation deficiency: an anatomic study. *AJNR Am J Neuroradiol* 1990;11: 431–439

Please see the Commentary on page 231 in this issue.